

# Dynamics of entangled polymers subjected to reptation and drift

## SUPPLEMENTARY INFO

Andrés R. Tejedor and Jorge Ramírez\*

*Department of Chemical Engineering,*

*Universidad Politécnica de Madrid,*

*José Gutiérrez Abascal 2, 28006, Madrid, Spain*

(Dated: February 11, 2020)

## SI. MEAN SQUARED DISPLACEMENT OF THE CENTER OF MASS

In the main text of the article, it is shown that the center of mass moves superdiffusively for significant drift values. In this section, we expand on this and derive an scaling argument to explain this superdiffusive behaviour and estimate the slope of this regime.

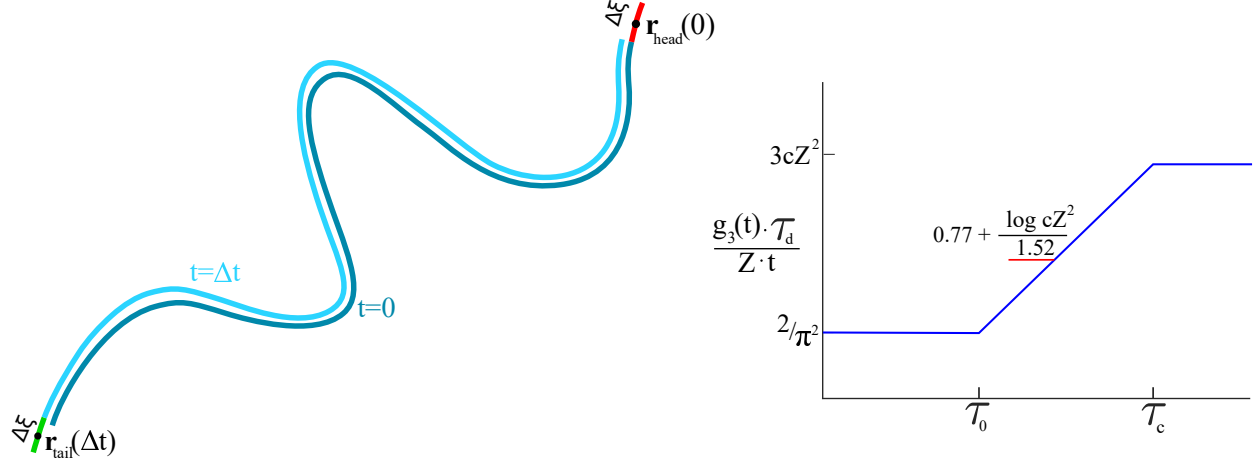


FIG. S1. Left: Schematic picture of a chain that reptates from head to tail evaluated at initial time (dark blue) and at a short time  $\Delta t$  (light blue). The destroyed tube segment is highlighted in red and the newly created tube segment in depicted in green. Right: Schematic plot of normalized mean squared displacement of the center of mass.

The superdiffusive regime can be explained by comparing the short and long times diffusive behaviour. At long times, it is easily showed (see Eq. (18) in the main text) that

$$g_3(t)\tau_d/Z/t \approx 3cZ^2. \quad (\text{S1})$$

By contrast, at very short times, a scaling argument can be used to extract the MSD of the center of mass. During a short time interval  $\Delta t$ , the tube reptates a distance  $\Delta\xi$ , where  $\langle \Delta\xi \rangle = 0$  and  $\langle \Delta\xi^2 \rangle = 2D_c\Delta t$  (see Fig. S1). We can compute the change in the center of mass between times 0 and  $\Delta t$  as:

$$\begin{aligned} \mathbf{r}_{\text{CM}}(\Delta t) - \mathbf{r}_{\text{CM}}(0) &= \frac{1}{Z} \int_0^Z ds (\mathbf{r}(s, \Delta t) - \mathbf{r}(s, 0)) \\ &= \frac{1}{Z} \left[ \int_0^{\Delta\xi} ds \mathbf{r}(s, \Delta t) - \int_{Z-\Delta\xi}^Z ds \mathbf{r}(s, 0) \right] \\ &= \frac{\Delta\xi}{Z} (\mathbf{r}_{\text{tail}}(\Delta t) - \mathbf{r}_{\text{head}}(0)), \end{aligned} \quad (\text{S2})$$

\* jorge.ramirez@upm.es

where the integrals between 0 and  $Z - \Delta\xi$  at initial time and between  $\Delta\xi$  and  $Z$  are cancelled as can be seen in Fig. S1. In the last equality, we have defined  $\mathbf{r}_{\text{tail}}(\Delta t)$  and  $\mathbf{r}_{\text{head}}(0)$  as the centers of mass of the newly created segment (depicted in green in Fig. S1) at  $t = \Delta t$  and of the destroyed segment (red) at  $t = 0$ , respectively, both with length  $\Delta\xi$ .

Using Eq. (S2), we can calculate the MSD of the center of mass as:

$$\begin{aligned} g_3(\Delta t) &= \langle (\mathbf{r}_{\text{CM}}(\Delta t) - \mathbf{r}_{\text{CM}}(0))^2 \rangle = \left\langle \frac{\Delta\xi^2}{Z^2} (\mathbf{r}_{\text{tail}}(\Delta t) - \mathbf{r}_{\text{head}}(0))^2 \right\rangle \\ &= \frac{\langle \Delta\xi^2 \rangle}{Z^2} \langle (\mathbf{r}_{\text{tail}}(\Delta t) - \mathbf{r}_{\text{head}}(0))^2 \rangle \approx \frac{\langle \Delta\xi^2 \rangle}{Z} = \frac{2D_c \Delta t}{Z} \end{aligned} \quad (\text{S3})$$

where we have used the fact  $\Delta\xi$  is independent of the current coordinates and orientation of the tube, and  $\langle (\mathbf{r}_{\text{tail}}(\Delta t) - \mathbf{r}_{\text{head}}(0))^2 \rangle \approx Z$ . In case the chain reptates from tail to head, a similar argument is applicable. Thus, at short times:

$$\frac{g_3(\Delta t) \tau_d}{Z \Delta t} \approx \frac{2}{\pi^2}. \quad (\text{S4})$$

Comparing equations (S4) and (S1), we see that the center of mass must undergo a superdiffusive regime in order to transition from the early time to the late time Fickian regimes. We can estimate the slope of the superdiffusive regime by taking into account the interval of time at which it can be observed. As discussed in the main text, a significant drift starts dominating the dynamics at  $\tau_0 = 0.01\tau_d/cZ^2$ . The final Fickian regime appears at the terminal time  $\tau_c = Z/c$ . Between  $\tau_0$  and  $\tau_c$ , the superdiffusive regime should be observable. In the right panel of Fig. S1 we show a schematic picture of  $g_3(t)$  properly normalized to show the superdiffusion, specifying the time range and expected limiting values. The slope  $m$  of the superdiffusive regime in logarithmic scale can be estimated as

$$m = \frac{\log 3cZ^2 - \log \frac{2}{\pi^2}}{\log \frac{1}{3cZ^2} - \log \frac{0.01}{cZ^2}} = \frac{\log \frac{3cZ^2 \pi^2}{2}}{\log \frac{100}{3}} \approx \frac{\log cZ^2}{1.52} + 0.77, \quad (\text{S5})$$

where all the times have been normalized by  $\tau_d$ . Therefore, during the superdiffusive regime the MSD of the center of mass has a dependence  $g_3(t) \propto t^\alpha$  with  $\alpha \approx \frac{\log cZ^2}{1.52} + 1.77$  for about two decades (100/3 as seen in Eq. (S5)).

## SII. ANALYTICAL SOLUTION FOR THE DYNAMIC STRUCTURE FACTOR.

In this part of the appendix, we explain how the dynamic structure factor has been computed. We start from its definition in Eq. (26) of the main text, and thus we firstly

solve the problem for  $\varphi(s, s'; t)$  given by the equation:

$$\frac{\partial \varphi}{\partial t} - c \frac{\partial \varphi}{\partial s} = D_c \frac{\partial^2 \varphi}{\partial s^2}. \quad (\text{S6})$$

Regarding the initial condition we assume that the primitive path conformation is Gaussian, and the boundary conditions can be directly adopted from the pure reptation problem [1] given that the drift is slow enough to allow the ends to explore all orientations:

$$\varphi(s, s'; 0) = \exp \left( -\frac{\mathbf{q}^2}{6} |s - s'| \right). \quad (\text{S7})$$

$$\begin{aligned} \left. \frac{\partial}{\partial s} \varphi(s, s'; t) \right|_{s=0} &= \frac{\mathbf{q}^2}{6} \varphi(s, s'; t) \Big|_{s=0}, \\ \left. \frac{\partial}{\partial s} \varphi(s, s'; t) \right|_{s=L} &= -\frac{\mathbf{q}^2}{6} \varphi(s, s'; t) \Big|_{s=L}. \end{aligned} \quad (\text{S8})$$

Assuming the solution can be split in a spatial and a temporal part, we can express  $\varphi(s, s'; t)$  as

$$\varphi(s, s'; t) = f(s, s') T(t). \quad (\text{S9})$$

Introducing above solution (S9) in the original equation (S6), the full problem is separated into the spatial

$$\begin{aligned} \frac{\partial^2}{\partial s^2} f(s, s') + \frac{c}{D_c} \frac{\partial}{\partial s} f(s, s') + \lambda_p^2 f(s, s') &= 0 \\ \left. \frac{\partial}{\partial s} f(s, s') \right|_{s=0} &= \frac{\mathbf{q}^2 a}{6} f(s, s') \Big|_{s=0} \\ \left. \frac{\partial}{\partial s} f(s, s') \right|_{s=L} &= -\frac{\mathbf{q}^2 a}{6} f(s, s') \Big|_{s=L}, \end{aligned} \quad (\text{S10})$$

and the temporal problem

$$\begin{aligned} \frac{\partial}{\partial t} T(t) + D_c \lambda_p^2 T(t) &= 0 \\ T(0) &= \exp \left( -\frac{\mathbf{q}^2 a}{6} |s - s'| \right). \end{aligned} \quad (\text{S11})$$

We start solving the problem (S10). The solution for the differential equation and which verifies the boundary conditions takes the form

$$\begin{aligned} f(s, s') &= \exp \left( -\frac{cs}{2D_c} \right) \\ &\times \sum_{p=1}^{\infty} \left\{ A_p \cos \left[ \frac{2\alpha_p}{L} \left( s - \frac{L}{2} + \nu \rho_p \right) \right] \right. \\ &\quad \left. + B_p \sin \left[ \frac{2\beta_p}{L} \left( s - \frac{L}{2} + \nu \sigma_p \right) \right] \right\}. \end{aligned} \quad (\text{S12})$$

The eigenvalues are obtained from the relations

$$\begin{aligned}
\alpha_p \tan \left[ \alpha_p \left( 1 - \frac{c\rho_p}{2D_c} \right) \right] &= \mu + \nu \\
\alpha_p \tan \left[ \alpha_p \left( 1 + \frac{c\rho_p}{2D_c} \right) \right] &= \mu - \nu \\
\beta_p \cot \left[ \beta_p \left( 1 - \frac{c\sigma_p}{2D_c} \right) \right] &= -\mu - \nu \\
\beta_p \cot \left[ \beta_p \left( 1 + \frac{c\sigma_p}{2D_c} \right) \right] &= -\mu + \nu,
\end{aligned} \tag{S13}$$

where

$$\mu = \frac{\mathbf{q}^2 a}{12}, \quad \nu = \frac{cL}{4D_c}. \tag{S14}$$

Latter variables show the magnitude of the scattering vector ( $\mu$ ) and the drift ( $\nu$ ). The original eigenvalues appearing in (S10) are related to  $\alpha_p$  as follows

$$\lambda_\alpha^2 = \left( \frac{2\alpha_p}{L} \right)^2 + \left( \frac{c}{2D_c} \right)^2, \tag{S15}$$

and analogously for  $\beta_p$ .

The phase of the eigenfunctions has been chosen in order to recover the pure reptation solution straightforwardly when the drift vanishes, and the terms with  $\rho_p$  and  $\sigma_p$  are required to assure the existence of the solution in (S13). Comparing with the original solution of Doi[1], the emergence of drift unfolds the eigenvalues equation, resulting on a system of two equations so  $\rho_p$  and  $\sigma_p$  are demanded by the system to be consistent. Apart from the condition that  $\alpha_p$  and  $\beta_p$  must be positive, in principle there are not any other constraint over the shift values. This unfolding makes the problem more challenging, since the couples of eigenvalues  $\alpha_p$ ,  $\rho_p$  and  $\beta_p$ ,  $\sigma_p$  may be not easy to find out.

Now the problem in time (S11) can be easily solved taking into account that eigenvalues are different for cosine and sine and using similar relations to that in the segmental motion problem. Therefore the solution is

$$T_\alpha(t) = \exp \left( -\frac{4D_c}{L^2} t (\alpha_p^2 + \nu^2) \right), \tag{S16}$$

and analogous form for  $\beta_p$ . The solution for the full problem is finally given by

$$\begin{aligned} \varphi(s, s'; t) = 2\mu \exp\left(\frac{c(s' - s)}{2D_c}\right) \times \\ \sum_{p=1}^{\infty} \left\{ A_p T_\alpha(t) \cos\left[\frac{2\alpha_p}{L} \left(s - \frac{L}{2} + \nu\rho_p\right)\right] \right. \\ \left. + B_p T_\beta(t) \sin\left[\frac{2\beta_p}{L} \left(s - \frac{L}{2} + \nu\sigma_p\right)\right] \right\}. \end{aligned} \quad (\text{S17})$$

Enforcing the initial condition (S11) and after some algebra, the coefficients  $A_p, B_p$  are computed to give

$$\begin{aligned} A_p = \frac{\frac{\mu^2 + \alpha^2 - \nu^2}{(\alpha^2 + (\mu - \nu)^2)(\alpha^2 + (\mu + \nu)^2)}}{\cos\left(\frac{2\alpha\nu\rho}{L}\right)\frac{\sin(2\alpha)}{2\alpha} + 1} \left\{ \cos\left[\frac{2\alpha}{L} \left(s' - \frac{L}{2} + \nu\rho\right)\right] \right. \\ \left. - \frac{2\nu}{\alpha^2 + (\mu - \nu)^2} \sin\left[\frac{2\alpha}{L} \left(s' - \frac{L}{2} + \nu\rho\right)\right] \right\}, \\ B_p = \frac{\frac{\mu^2 + \beta^2 - \nu^2}{(\beta^2 + (\mu - \nu)^2)(\beta^2 + (\mu + \nu)^2)}}{\cos\left(\frac{2\beta\nu\sigma}{L}\right)\frac{\sin(2\beta)}{2\beta} - 1} \left\{ \sin\left[\frac{2\beta}{L} \left(s' - \frac{L}{2} + \nu\sigma\right)\right] \right. \\ \left. - \frac{2\nu}{\beta^2 + (\mu - \nu)^2} \cos\left[\frac{2\beta}{L} \left(s' - \frac{L}{2} + \nu\sigma\right)\right] \right\} \end{aligned} \quad (\text{S18})$$

The solution for the dynamic structure factor is finally obtained from  $\varphi(s, s'; t)$  integrating in  $s$  and  $s'$  and can be seen in the main text.

### SIII. CONTOUR LENGTH FLUCTUATIONS.

We dedicate this section of the appendix to study the consequences of contour length fluctuations (CLF) in depth. First, we explore how the homogeneous drift modifies the escape of the tube comparing with the case of pure reptation with drift. Secondly, we determine how the length and fluctuations are affected by the active monomer when dragging the chain from one of its ends.

#### A. Reptating Rouse chain with homogeneous drift

In the analysis of homogeneous drift with CLF, we observed that the dynamics of the chain in the tube segment was not trivial with respect to the pure reptation solution with drift  $\psi(s, t)$ . The time at which we measured  $\psi^{CLF}(s, t^*)$  is normalized in the case without

drift as described in the main text. However, for a given  $c$  the pure reptation solution with drift decays faster in some parts whereas in other times the escape is slower. In order to clarify this effect in more detail, in Fig. S2 we compare the tube survival functions with and without CLF, for several values of the drift.

For small drift values ( $cZ^2, cZ_{eff}^2 = 4^{-3}, 4^{-2}$ ) both functions decay equally fast, as expected from our choice of the times  $t'$  and  $t^*$ . For intermediate drift values ( $cZ^2, cZ_{eff}^2 = 4^{-1.5}, 4^{-1}, 4^{-0.5}$ ), at short times, pure reptation destroys the tube faster than reptation with CLF, but in the vicinity of the terminal time, CLF helps to destroy the tube faster. For large drifts ( $cZ^2, cZ_{eff}^2 = 4^0$ ), the escape from tube occurs much faster by pure reptation.

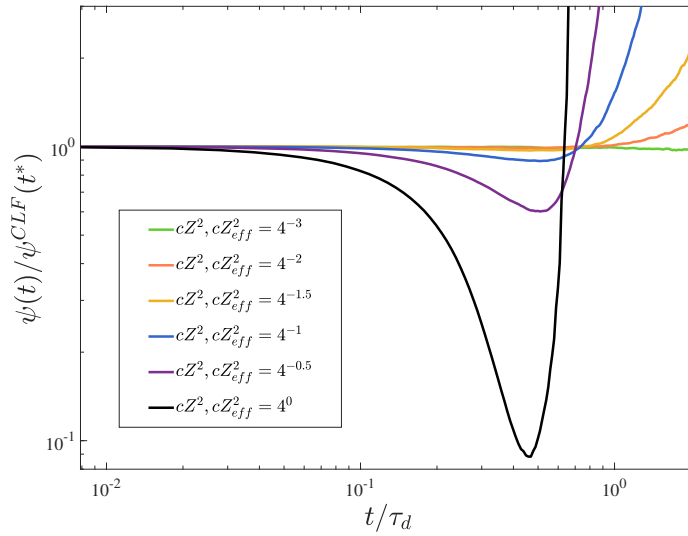


FIG. S2. Relation between  $\psi(t)$  and  $\psi^{CLF}(t)$  with respect to time  $t$ , for different values of the drift and for a system with  $Z = 16$  and  $Ns = 2$ .

To explain this phenomenon first we want to recall some important issues involved: (i) The value of the drift for pure reptation is smaller than the drift in CLF so that  $Z_{eff} < Z$  and we have assumed the same scaling behaviour; (ii) The part of the curves after its relaxation time are not reliable since the precision in the simulation decrease. With this in mind we recall the three mechanisms that contribute to the tube destruction. The fluctuations, that governs the dynamics at very short times ( $t^{1/4}$ ), the diffusion along the tube ( $t^{1/2}$ ) and finally the drift, which mainly affects at long times ( $t$ ).

It is reasonable to expect the faster decay of  $\psi^{CLF}(t)$  with respect to  $\psi(t)$  ( $\psi(t)/\psi^{CLF}(t) > 1$ ) for long times since its drift  $c$  is bigger. However, the regime in which the pure reptation evolves faster than with CLF ( $\psi(t)/\psi^{CLF}(t) < 1$ ) for the largest drifts can seem counterin-

tuitive but this can be explained since  $t > t^*$ , and for that reason the drift is more effective in the decay of  $\psi(t)$ , *i.e.*, in our choice for measuring the time, the survival function for pure reptation is measured in later times.

## B. Head propelled polymer

Here we investigate how the end-to-end vector  $\langle \mathbf{R} \rangle$  is modified by the presence of the drift in the head. With this purpose we introduce the linking vectors  $q_i = r_i - r_{i-1}$  and using the equations of motion, the evolution can be expressed as

$$\frac{d\mathbf{q}}{dt} = A\mathbf{q} - \mathbf{c}, \quad (\text{S19})$$

where for the head propelled polymer the term of the drift is slightly modified:

$$A = \begin{pmatrix} 2 & -1 & & \\ -1 & \ddots & \ddots & \\ & \ddots & \ddots & -1 \\ & & -1 & 2 \end{pmatrix}_{N \times N} \quad \mathbf{c} = \begin{pmatrix} \frac{-1}{N_e} \\ 0 \\ \vdots \\ 0 \\ \frac{1}{N_e} + \frac{c\pi^2}{N_e} \end{pmatrix}, \quad (\text{S20})$$

and  $\mathbf{q}$  contains the link vectors  $q_i$ . In the equilibrium state, the binding vectors have a constant length on average, and then averaging Eq. (S19) we get

$$\langle \mathbf{q} \rangle = A^{-1} \mathbf{c}. \quad (\text{S21})$$

The average length of each link is easily computed by calculating the inverse of the matrix  $A$ :

$$\langle q_i \rangle = \frac{1}{N_e} \left( 1 + \frac{c\pi^2 i}{N_e} \right) \quad i = 1, \dots, N. \quad (\text{S22})$$

The latter expression for the binding vectors is useful to set the upper limit for  $c$  in the main text. Finally we use this relation, to compute the end-to-end vector:

$$\langle \mathbf{R} \rangle = Z \left( 1 + \frac{\pi^2 c (N+1)}{2 N_e} \right). \quad (\text{S23})$$

---

[1] M. Doi and S. Edwards, *The Theory of Polymer Dynamics*, Vol. 73 (Oxford University Press, 1988).